

# Strain Measurement With Fiber Mach-Zehnder Interferometer Using Spatial Phase Measurement Techniques

Kamal Rani, Ajay Shankar

**ABSTRACT:** Fiber Mach-Zehnder interferometer (MZI) provides sensing applications with optical fiber for measurements like stress, strain and temperature. Over time MZI has been realised and studied with a beam splitter, mirror and detectors and has been improved using couplers, single mode fiber and detectors as well as inline fiber MZI. In these MZI setup input light is splits into two equal parts which then propagates separately through both reference and measurement fibers. With this set up we demonstrated producing stable detector width compensated fringes suitable for phase measurement due to strain in measuring arm applying spatial phase measurement (SPM) techniques for strain sensor applications.

**Index Terms:** Mach Zehnder Interferometer, Fiber Sensor, Coupler, Spatial Phase Measurement.

## 1. INTRODUCTION

Strain measuring techniques became very attractive and powerful with the arrival of fiber optic sensors because it is resistant to electromagnetic interference (EMI), specifically in noisy environments. A single mode fiber optic strain metrology system is developed by Butter and Hocker (1978) but the limitations of the system was fiber management and the manual fringe count [1]. In this paper single mode fiber optic interferometer for strain measurement system has been studied using spatial phase measurement concept used in phase stepping interferometry. The Strain is analyzed by fiber targeted probe which is mounted on specimen like a rod. Due to displacement of target strain is generated in fiber simultaneously this cause a phase shift which is a result of variation of optical path length (OPL) in one of the fibre arms of interferometer. A tremendously high resolution to the measurand is offered by the interferometric fiber sensors. Hence the precision of the measurement to be determined by taking out the phase information from the interferogram. Diversity in the approaches have been validated for phase extraction from the interferogram. Phase stepping methods have been used since 1974 and have been further investigated by many researchers. Many different variants of these phase-stepping algorithms have been developed, such as three-frame, four-frame, five-frame and the "2+1" techniques [2-4]. In the present study for extraction of information from the interferometric fringes we are using a four-step phase shifting technique for intensity measurement of an interferometric pattern at sundry phase shifts. Block diagram for optical design of fiber interferometer is given in Fig.1.

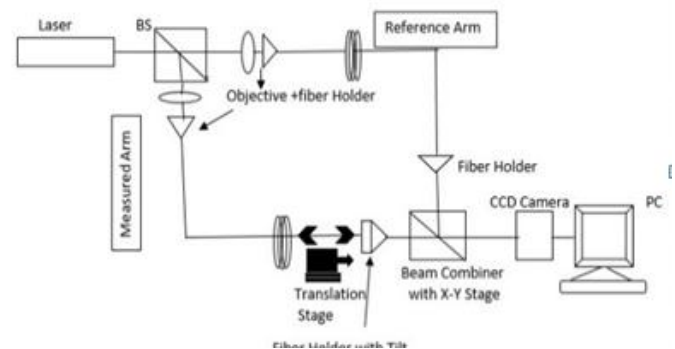
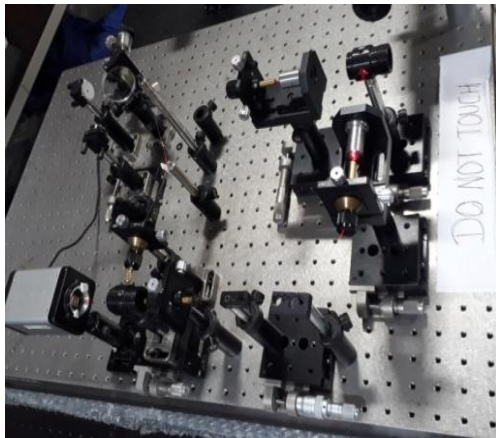


**Fig.1:** Diagram of Optical Design of Fiber Interferometer

### I. FIBER OPTIC INTERFEROMETRIC SET UP

In a Mach-Zehnder interferometer (MZI), the light is split into two beams and split light travel into two fiber arms in its fiber MZI configuration. Fig.2(a) presented our Experimental setup for Fibre MZI. We used a HeNe laser at 632.8nm as a light source, cube beam splitter is used to split the output in two beams which are focussed and launched into two identical end prepared single mode optical fibers. Some portion of the sensor arm fiber (40mm) is fix on two rods by epoxy. Good end prepared single mode bare fiber is chosen over other fibers because effects due to jacket and bad fiber end has to be avoided. One rod movable in translation stage (Newport made, model M-423 Series with 25 mm travel range) and other one has been stable on aluminium base plate and as seen in fig.2 (b). The reference arm has been inaccessible from outer perturbations the fiber has been given strain using micro-movement with a differential micrometre.



(a)



(b)

**Fig.2:** (a)Set Up for Fiber Mach-Zehnder Interferometer  
(b) Probe Design

The two beams are again recombined by overlay at the inside of the beam combiner and form an interference pattern. The most stringent requirement was to generate stable straight line fringe pattern having desired fringe width meeting out criteria for detector width compensation which is primary condition for using the concept of spatial phase measurement (SPM) requiring nearly perfect tuning of fringe width with a detector pixel dimension. This pattern is detected using a detection system having a CCD camera which gives output to a NI-PCI frame grabber and then further processed with VISION/LabVIEW software on a PC. We acquired image from CCD using features of PCI-1407 and VISION tools and once one fringe width matched four pixel width a quadrature signal values were generated in real-time. The phase information from the fringe pattern of the interferogram is extracted by using an appropriate image processing algorithm and for the measuring change in path length of fiber a fiber strain probe has been used as shown above.

The phase  $\phi$  of the fringe patterns can be measured using:

$$\phi(x, y) = \tan^{-1} \frac{\Im[c(x, y)]}{\Re[c(x, y)]} \quad (1)$$

where  $\Im[c(x, y)]$  and  $\Re[c(x, y)]$  are intensity values difference from fringe pattern at fixed phase interval desired by a particular algorithm.

The phase measured via four quadrature values which are resulting from the fringe pattern for our 4 point phase algorithms with 90 degree phase shift steps, fringe width

must exactly match width of 4 pixels, and then adding every 4<sup>th</sup> pixels of each image frame we generate the four quadrant values with significant values making effects of noise negligible. After achieving the proper quadrant values we calculated the phase of fringe pattern. On any change in condition of measuring fibre compared to reference fibre a  $\phi$  phase shift between the reference and measurement signals were measured in real time wrapped between  $-\pi/2$  to  $\pi/2$  using LabVIEW programming features.

## 2. SENSOR PRINCIPLE AND MATHEMATICAL MODEL

The intensity of Mach-Zehnder interferometer (MZI) is written as:

$$I = I_1 + I_2 + 2\sqrt{I_1 I_2} \cos(\omega\tau - \phi) \quad (2)$$

Here the intensities of the two arms are  $I_1$  and  $I_2$ , time difference of the interfering beam is  $\tau$  and the phase difference between the beams is  $\phi$ . The transduction mechanism by which a fiber optic axial strain produces a phase change in the optical path length. The phase  $\phi$  of the light can be expressed

$$\phi = \beta L \quad (3)$$

In a length  $L$  of sensing fiber, the phase variation  $\Delta\phi$  induced by applying axial strain on the fiber length ( $L$ ) resulted mainly from the physical length change ( $\Delta L$ ) and change in waveguide propagation constant ( $\Delta\beta$ ).

$$\Delta\phi = \beta\Delta L + L\Delta\beta \quad (4)$$

Here  $\beta = n_{\text{eff}} k_0$ , where  $n_{\text{eff}}$  is an effective refractive index and  $k_0$  is the free space wave propagation constant. The value of  $\beta$  is similar to  $n k_0$  because the core and cladding indices are differed by the order of 1%. A mechanical force smeared to the fiber results in changing in  $n$  and  $L$ , and, therefore, in  $\phi$  the equivalent expression relating these changes are shown in Eq (5). The resultant strain  $\epsilon$  is the length change  $\Delta L$ , divided by the initial length  $L$  ( $\epsilon = \Delta L/L$ ).

We assume that there is no variation in the refractive index of the fiber. When we apply the strain on the fiber only its length changes. Therefore we calculate the overall strain induced by phase change from equation 4.

After expanding:

$$\Delta\phi = L\epsilon\beta \left[ 1 - \frac{n_{\text{eff}}^2}{2} [\rho_{12} - (\rho_{12} + \rho_{11}) \epsilon] \right] \quad (5)$$

For typical glasses  $n_{\text{eff}} = 1.46$ ,  $\nu = 0.16$  (Poisson's ratio of fiber material),  $\rho_{11} = 0.113$ ,  $\rho_{12} = 0.252$  are strain optic coefficients for quartz fiber,  $\beta = 2\pi n_{\text{eff}} / \lambda$ ,  $\lambda$  is sensing wavelength (632.8nm for He-Ne Laser).

Substituting the above value in equation 5:

$$\Delta\phi = L\epsilon(1.15 \times 10^7) \quad (6)$$

$$\text{and } \epsilon = \frac{\Delta\phi}{L(1.15 \times 10^7)} \quad (7)$$

Therefore 1 fringe for a phase change  $\Delta\phi$  of  $2\pi$  radian and strain  $\epsilon$  is the  $\Delta L/L$  then equation 6 is used to give change in sensing length ( $\Delta L$ ) which is  $0.546\mu\text{m}$  per fringe and theoretically strain generated  $12.5\mu\epsilon$  for the sensing length 40 mm expected for our experiment.

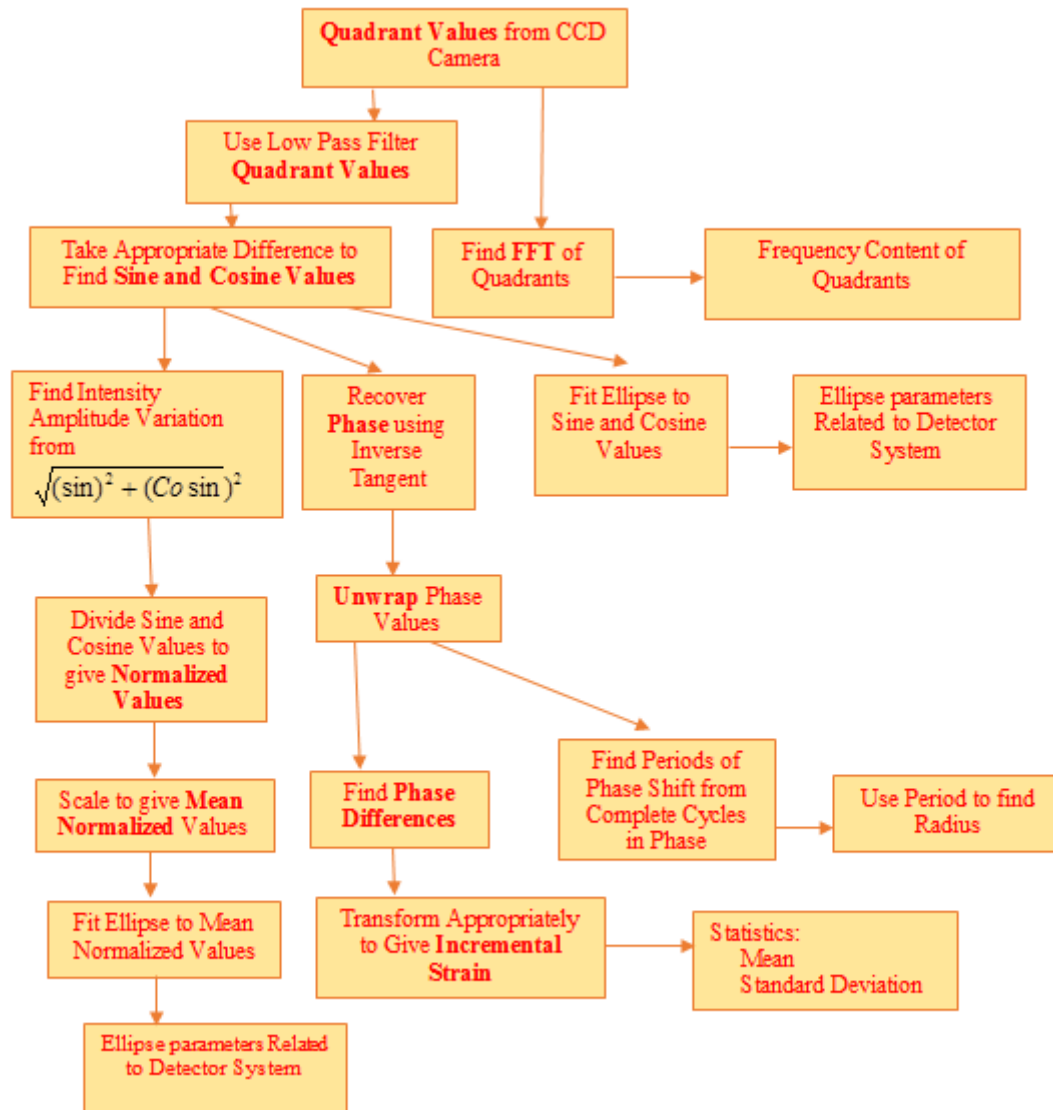


Fig.3. Flow Chart for Data Analysis in Real Time

### 3. DATA ANALYSIS AND FLOW CHART

Data analysis steps used by us are shown in the flowchart (Fig.3). This data analysis is carried out in real-time so we have the greater quantity of data as well as better quality of data. For these reasons it is possible to obtain significantly more useful and reliable information about the Mach-Zehnder interferometer system from the real time data.

### 4. FOUR POINT PHASE-STEPPING TECHNIQUE

As this interference fringe intensity relation contains three unknown quantity which are the intensities of two interfering beams and therefore a measurement of phase from the interference pattern requires at least three intensity values must be known at three sets of a known phase shifted pixel. There are a number of algorithms suggested getting such phase information all having their own merits and demerits.

As discussed by Schmit [5-7] for spatial phase measurement (SPM), the N-Point techniques use N adjacent detector elements (pixels) of an array detector. The Phase shift between these detector elements by the spatial positioning of that element in any fringe pattern has been extensively studied by them. The most common technique for recovering the phase, utilize a phase shift of  $90^\circ$  between the 4 intensity signals which correspond to detector elements chosen to be one-fourth of the interference fringe width. The algorithm is given as

$$\phi = \tan^{-1} \left( \frac{I_3 - I_1}{I_0 - I_2} \right) \quad (8)$$

This inverse tangent will give a phase value that ranges from  $-180$  to  $+180$  degrees. Because of this limited range of phase values, discontinuities in the recovered phase values will exist when the phase either passes beyond  $180$  degrees or below  $180$  degrees. To avoid erroneous large displacements due to these discontinuities, it is necessary to remove them using a phase unwrapping technique that

identifies a discontinuity and adds or subtracts 360 degrees to the recovered phase value, which will remove the discontinuity.

#### Phase Unwrapping

The path of phase unwrapping is oriented according to the parameter map and its value is determined by each pixel in wrapped phase pattern. This basic operation used for removing discontinuity points during phase detection. Since the arctangent ranges from  $\pi$  to  $\pi$  and the phase value provided from phase unwrapping methods will have  $2\pi$  phase discontinuities.

$$\Phi(x, y) = \phi(x, y) + 2\pi k(x, y) \quad (9)$$

Phase unwrapping is used to obtain a continuous phase distribution.

Where  $\phi(x, y)$  = wrapped phase,

$\Phi(x, y)$  = unwrapped phase,

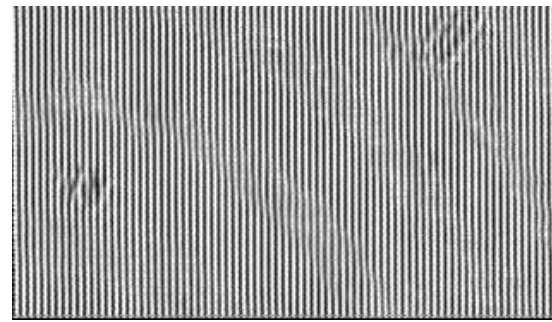
$k(x, y)$  = integer number to represent fringe orders.

The key to a phase unwrapping algorithm is rapidly and correctly finding  $k(x, y)$  for each pixel in the phase map. On the other side the theoretical sense this method is straightforward and simple, in real time phase contains discontinuities and additive noise which may delay the phase unwrapping process.

## 5. RESULTS AND DISCUSSIONS

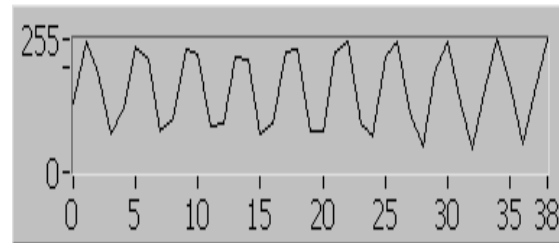
For real-time strain measurement experiments entire processing was done using LabVIEW/ VISION control which uses a continuous image acquisition mode with 5 to 10 buffers from which images are extracted one by one in real time for processing. The pixel grey intensity values are used to calculate various parameters by use of LabVIEW programming features. Thereby continuous data are generated for onward image cum data processing. The matrix of the grey intensity level of various pixels was broken into four sub-matrix equivalents to four quadrants as desired using LabVIEW function.

We used the region of interest tool available with LabVIEW to select the best part of the fringe pattern having horizontal pixel in multiple of four from the full frame image shown in Fig. 4. This not only speeds up the process but has good effect on noise value in signal, increasing the SNR also. Exact quadrature signal is generated when periodicity of fringe is come out in 4 pixels per fringe width which is monitored and confirmed in LabVIEW window simultaneously to achieve the correct periodicity of fringes. The phase value measured is wrapped between  $-\pi$  to  $\pi$ . Four point phase retrieval technique is used for phase extraction. Using this technique phase can be retrieved from the quadrant values generated out of the fringe pattern from the strain measuring interferometer from the spatial fringe pattern. In Fig. 5(a) detected wrapped phase is shown which contains discontinuity of phase signal, which has very large noise during phase calculation. So discontinuity from phase data is removed from phase unwrapping algorithms design in LabVIEW shown in fig. 5(b). After removing discontinuity from phase data we calculate the change in phase which can be used for strain measurement with high accuracy.

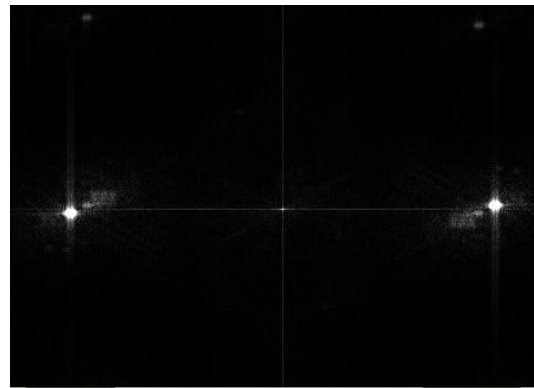


(a)

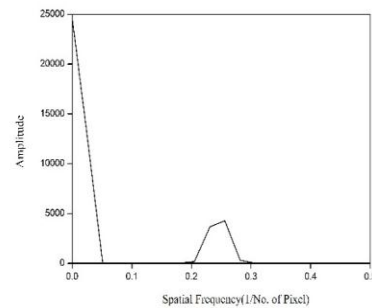
Line Profile



(b)

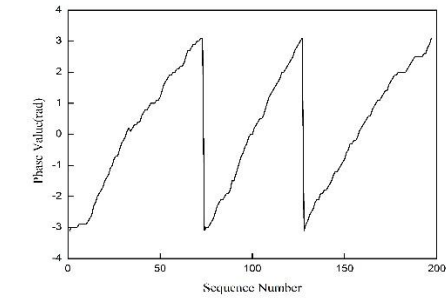


(c)

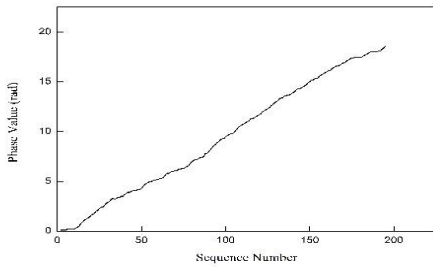


(d)

**Fig.4:** (a) Fringe Pattern selected using Region of Interest (ROI) (b) line profile of image (c) FFT of image (d) Periodicity of fringe pattern using FFT With LabVIEW



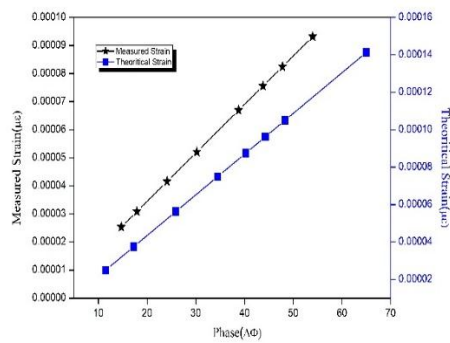
(a)



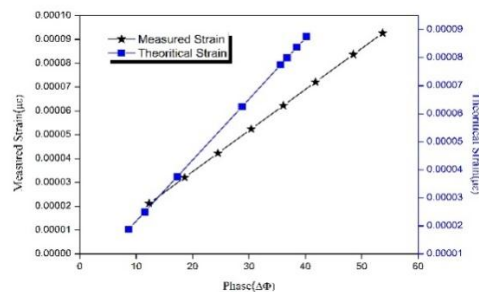
(b)

**Fig.5** (a) Wrapped phase (b) Unwrapped phase

This work He Ne source (632.8nm) was used and experiments were performed on a vibration isolation table and simultaneously the interference patterns were captured under the strained conditions in measuring fiber arm of Sensor designed in this work. It consists of 40 mm sensing fiber length corresponding to minimum strain ( $\Delta L/L$ ) is induced  $30\mu\epsilon$  for change in sensing length by  $1.5\mu\text{m}$ . The incremental change in phase is higher than than the expected value for initial stress condition where effect if a residual jacket or epoxy dominates and less in case of full loaded stress as shown in fig 6(a) and 6(b).

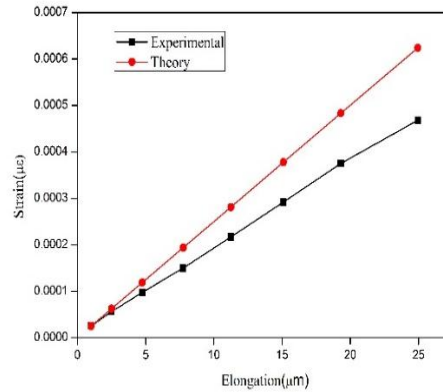


(a)

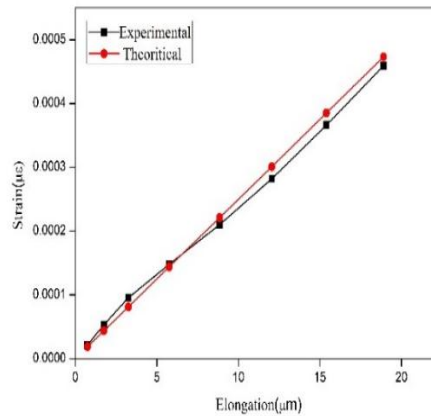


(b)

**Fig.6:** (a) Related Incremental phase vs. strain graph for starting stress Fig.6 (b) Related Incremental phase vs. strain graph for full stress



(a)



(b)

As shown in Fig. 7(a) and 7(b) cumulative displacement and cumulative strain have been calculated for unstressed and stressed fiber.

**TABLE I**  
STATISTICS FOR REAL-TIME STRAIN MEASUREMENT BY USING SINGLE MODE FIBER MACH-ZEHNDER INTERFEROMETER

	Initial Stress	Full loaded Stress
Experimental strain generated(micron)	0.00046	0.00045
Standard Deviation Error for cumulative strain(micron)	0.00050	0.0012
Standard Deviation Error for incremental strain(micron)	0.0013	0.0007
Cumulative Displacement(micron)	24.95	18.9

This experimental result shows that strain measured is less than the expected value. 25- Micron strain has 2 fringe shift of  $4\pi$  phase change with a change in length 1 micron for initially when stress was applied on sensing fiber. At same condition when further stress is applied on sensing fiber change in length is 0.75 microns for  $4\pi$  phase shift 21 micron strain is measured. This result is in the presence of noise in the fringe patterns and detector noise and further improved by developing an adaptive filter.

**TABLE II.**  
T-TEST: CUMULATIVE STRAIN FOR FULL LOADED  
STRAIN VS INITIAL STRAIN

	Variable 1	Variable 2
Mean	0.000210224	0.000204487
Variance	2.49419E-08	2.40573E-08
Observations	8	8
Pearson Correlation	0.999934218	
Hypothesized Mean Difference	0	
Df	7	
t Stat	4.846807084	
P(T<=t) one-tail	0.000931568	
t Critical one-tail	1.894578605	
P(T<=t) two-tail	0.001863135	
t Critical two-tail	2.364624252	

As we have conducted independent samples t-test for initial and full loaded strain measurement from single mode fiber MZI. There is a significant difference between measured strain with initial and full loaded there result suggest that the strained fiber have more measured value of strain and closure to computed value as compared to strained start condition fiber w.r.t. to change in displacement introduced experimentally. As shown in fig.7 (b) that strained fiber have more sensitivity on changes in the strain as compared to expected strain w.r.t to change in displacement.

## CONCLUSION

Data acquired from fringe pattern can be easily processed using VISION/LabVIEW tools to generate quadrant signal for phase measurement once stable detector width compensated fringe are produced. The spatial phase measurement (SPM) is an effective phase is measurement by the four point phase stepping Interferometric technique which is one the most suitable and competitive technique for this FMZI sensor for strain measurement setup. This set up can be used for strain measurement and this interferometric sensor detect the low value of strain however to minimize residual jacket material and epoxy effects measuring arm should be used in moderate stress conditions.

## REFERENCES

- [1] C. D. Butter and G. B. Hocker, "Fiber optics strain gauge," Appl. Opt., vol. 17, pp. 2867-2869, Sep. 1978.
- [2] J. H. Bruning, D. R. Herriott and J. E. Gallagher, "Digital Wave front Measuring Interferometer for Testing optical Surfaces and Lenses," Appl. Opt., vol. 13, pp. 2693-2703, Nov. 1974.
- [3] James C. Wyant And Katherine Creath, "Advances In Interferometric Optical Profiling," Int. J. Mach. Tools Manufact., vol. 32, No. 1/2, pp. 5-10, Feb. 1992.

- [4] K. Creath, and J. Schmit, "Errors in Spatial Phase-Stepping Techniques," in Interferometry '94: New Techniques and Analysis in Optical Measurements: 16-20 May 1994, Warsaw, Poland, Proc. SPIE vol. 2340, pp. 170-177, Dec. 1994.
- [5] J. Schmit, K. Creath, and M. Kujawinska, "Spatial and Temporal Phase-measurement techniques: a comparison of major error sources in one dimension", Interferometry: Techniques and Analysis, SPIE vol. 1755, pp. 202-212, Feb. 1993.
- [6] K. Creath and J. Schmit, "N-Point Spatial Phase measurement Techniques for Non-destructive Testing", Opt. and Lasers in Eng., vol. 24, pp. 365-379, May 1996.
- [7] J. Schmit and K. Creath, "Extended averaging technique for derivation of error-compensating algorithms in phase shifting Interferometry", Appl. Opt., vol. 34 (19), pp. 3610-3619, July 1995.

Kamal Rani, completed B.Tech in Electronics And Communication Engineering from Maharshi Dayanand University, Rohtak in 2009. Completed M.tech in Optical Engg from Guru Jambheshwar University of Science and Technology, Hisar in 2011. Currently pursuing Ph.d in Optical Engg, Dept of Physics from Guru Jambheshwar University of Science and Technology, Hisar. Her research interests include fiber based interferometer sensor. Dr. Ajay Shankar, Completed M.tech from Delhi. Completed Ph.d from Delhi University. Currently working as an Associate Professor in dept. Of physics, GJUS&T, Hisar. Fields of Interest are Sensor, Interferometry, and Imageprocessing.